Preparation and investigation of fulvic acid and its metal derivative complexes with application

Abdou. S. EL-Table*[1] ;Magdy. A. Wassel[2] and Mahmoud. M. Arafa[1]
*[1]Department of Chemistry , Faculty of Science , El-Menoufia University, Shebin El-Kom, Egypt .
[2]Department of Chemistry, Faculty of Science, El-Azhar University , Nasr city, Cairo, Egypt

Abstract: This work was focused on the preparation of fulvic acid and its derivative, also characterization using analytical techniques as elemental analysis (C, H, N and M) spectral techniques as IR, mass spectra. The preparation of metal complexes by reaction of fulvic acid derivatives with metal ions such as : **Cu(II), Co(II), Cd(II), Ca(II), Ni(II),Mn(II), Fe(II) and Mg(II).** The characterization of the prepared solid complexes using analytical techniques , spectral techniques as IR, UV-VIS, H-NMR, ESR and thermal techniques as TGA and DTA. Also illustrated its applications (agriculture and biomedical).

Keywords: fulvic acid , metal complexes , analytical , spectral techniques ,application

INTRODUCTION

1. DEFINITION OF FULVIC ACID

Fulvic acid is a part of the humic structure in rich composting soil. It is an acid created in extremely small amounts by the action of millions of beneficial microbes, working on decaying plant matter in a soil environment with adequate oxygen. It is of low molecular weight and is biologically very active.

2. APPLICATIONOF HUMIC SUBSTANCES

Humus represents one of the greatest carbon reservoirs on Earth. So far, industrial applications of humus and humus-derived products are rare. On the contrary, the usage of coal was more abundant and essentially, it constituted the basis of the chemical industry in the second half of the 19th century and the first half of the 20th century. Petroleum was also an application and it was regarded as the main raw material for the chemical industry of the 20th century. Nowadays, applications of HS can be divided into four main categories: agriculture, industry, environment and biomedicine.[1]

3. AGRICULTURE APPLICATIONS

HS and FA play an important role from the agronomical point of view. They influence significantly the quality and productivity of the soil. In addition to
the improvement of the soil.s physical properties and moisture conditions mentioned above, HS also show a high base exchange capacity, which is important for soil fertility. Currently, humic materials are used as additivesin fertilizers. Different salts of humic substances, such as calcium humate, were used to increase soil fertility. The fertilizing effect of sodium humate on plant leaves has been described. Ammonium humate was also found to have a significant growth-stimulating effect. The characteristics of and applications for humic acids extracted from different compost have also been studied. [1]

The growth-promoting effect of humic substances has been observed by many investigators and humates are often part of different preparations for growth-improvement of plants. Productivity of soil is increased by different ways in the presence of humic materials. The indirect effects of humic substances are very important as they integrate iron to the chelates and make it available to plants. Another role of humic substances lies in the enhancement of the quality of soils when they are very poor in organic matter. Recent research shows that humic acid can be used as farm animal feed thanks to its growth-promoting effect.[1]

4. ENVEROMENTAL APPLICATIONS

Natural organic colloids (humic and fulvic acids) are important because they form water-soluble complexes with many metals including radionuclides. These organics may therefore be important as radionuclide transport agents through the environment. It is known that the presence of humic substances in natural waters can influence the uptake of radionuclides by natural solids and thus their migration to surface and ground waters. The main task of humic substances in environmental chemistry is to remove toxic metals, anthropogenic organic chemicals and other pollutants from water. Ion-exchange materials based on calcium humate were found suitable for the removal of such heavy metals as iron, nickel, mercury, cadmium and copper from water and also to remove radioactive elements from water discharges from nuclear power plants. [1]

Their selective binding capabilities are also exploited for the destruction of munitions and chemical warfare agents. Humus-based filters have been developed for sewage purification, with many applications. The filters are useful to clean chromate smelter wastewater, to remove oil and dyes from wastewaters and aquatic systems, to filter urban and industrial wastewaters, to remove pesticides from

sewage and to remove phenol from water. Humus-containing materials have been also utilized for sorbing gases, e.g. the removal of waste gases from an animal carcass rendering plant. Slightly modified humates can be applied to remove hydrogen sulfide and mercaptans from municipal gas supplies, and sulfur dioxide from stack gases. [1]

Different groups of compounds such as herbicides, fungicides, insecticides, nematicides, dioxins and also some pharmaceutical products like estrogenic compounds were determined as possible environmental endocrine disruptors. Thanks to their ability to adsorb organic pollutants from the environment, humic substances were found to be useful to remove those contaminants from water, soil and sewage sludges. The complex nature of the interaction between HS and xenobiotics and their influence in the environmental quality (water, soil, and atmosphere) has been studied by different authors. [1]

The study of the acido-basic and complexation properties of HAs with several inorganic and organic compounds has attracted increased attention due to their influence on many aspects of soil and water quality, and industrial processes. found that some inorganic and/or organic pollutants were strongly complexed (bound) only with some of the HAs components. As a consequence of such interaction quite stable entities of the supramolecular kind were formed. The interactions between humic materials and microorganisms have been intensively studied for the past 30 years. It was found that fermenting bacteria could reduce humic substances. [1]

This fact has significant implications for the autecology of anaerobic bacteria in soils and sediments. The cumulative production of acetate during this process seems to be energetically advantageous for fermenting bacteria. Utilization of humics as the energy supply for specific bacteria, fungi and higher microorganisms was studied by many investigators but it was noted that they can not exploit humic materials as a food source.[1]

5. BIOMEDICAL APPLICATIONS

Of great interest is that hospital studies show that difficult viral respiratory illnesses common in children are readily resolved with fulvic acid dietary supplementation. Fulvic acid is a humic extract common to rich organic humus soil and also certain ancient plant deposits. Many medical studies show that humic substances, especially fulvic acids, have the power to protect against cancer and related cancer-causing viruses. Studies often show reversal of deadly cancers and tumors using special humic substance therapies.[1]

6. METAL COMPLEXES DERIVED FROM FULVIC ACID

Complex formation reactions with the interaction of fulvic and humic acids with zinc and iron ions in a model aqueous system. The complexing ability of humic acids was experimentally proved to be much higher than that of fulvic acids. The complexing ability of fulvic acids is found to decrease over time. The dependence of the complexing ability of heavy metals on the types of ion and humic substances and the proportions of components in the solution is examined. The obtained experimental results on the occurrence forms of heavy metals were compared with their theoretical estimates calculated for natural water bodies.[2]

Ions of heavy metals (HM) in aquatic systems are involved in existing migration cycles. They migrate, accumulating in all components of the aquatic environment: in the water itself, suspended matter, bottom sediments (BS), and living organisms [3,4]. This disturbs the interactions in aquatic ecosystems, affects their structure, and causes the appearance of techno genic geochemical anomalies. A specific feature of HM is the fact that they with stand biodegradation and can accumulate in large amounts in water, aquatic organisms, and BS [3].

It is common knowledge that HM ions are most toxic; therefore, data on not only on their total content, but also on the forms of occurrence are of great importance. Freshwater ecosystems have some buffer capacity with respect to HM by which many researchers [3-5] understand an index, which characterizes the amount of the metal that does not significantly disturb the natural functioning of the entire aquatic ecosystem. The organic matter of natural waters can bind with the HM entering the system, thus reducing their toxic properties. [6, 7]

OM in water consist predominantly (up to 80%) of humic substances (HS), represented by high molecular, dyed, poly functional compounds [7]. The natural–climatic zones feature various ratios of fulvic (FA) and humic (HA) acids.. Owing to their different composition and chemical intramolecular reactions in the aquatic environment, humic matter fractions have different complexing abilities [6,7]. The ions of heavy metals also differ from one another in the complexing ability. The objective of this study was to examine the processes of complexation between HM substances and different HM ions. Experimental results were compared with observations and theoretical estimates of their concentrations in natural water bodies.[7]

The most important reactions for HM ions in natural aquatic systems are complexation processes with FAs and HAs dominating OM in water and soils. The understanding of HM ion migration mechanisms directly depends on the knowledge about the interaction between metal ions and humic substances. The obtained experimental data showed that an increase in HS amount is accompanied by an increase in complexation with HM ions; the affinity of HM for complexation with HS can be different; the complexation activity of FAs decreases over time; the complexing ability of related Fe ions—Fe(II) and Fe(III) may have different complexing ability; the complexing ability of bivalent Zn is the least; FAs can concentrate HMs in the aquatic phase, thus

facilitating its migration. HAs feature greater activity in binding HMs, but lower migration capacity.[7]

Humic substances (HS) are complex molecules characterized by high molecular weight and high chemical heterogeneity. In order to have a deeper understanding of these molecules, there is need to synthesize humic
acids (HA) and fulvic acids (FA) with determined functional groups. In this paper we report a systematic study on the synthesis of both HA and FA as a function of pH and nature of the functional groups. HA and FA with two functional groups (phenolic and carboxylic) has been synthesized through polymerization of catechol and acetic acid, calibrated by dialysis with membranes of 500, 1000 and 10000 MWCO (Molecular Weight Cut Off) and characterized using two spectroscopic measurement techniques (ATR-FTIR and UV-Visible). Our synthesis technique is inexpensive and simple to undertake. There is no saturation of the reaction medium with oxygen.[8]

Humic substances (HS) are complex and ill-defined polydispersed mixtures of heterogeneous polyelectrolytes that are of importance in natural environment due to their role in regulating ion concentration in solution. They are described as refractory dark-coloured, heterogeneous organic compounds produced as by-products of microbial metabolism. They are one of the most widely distributed organic materials on Earth. Formed by the random condensation of the degradation products of plants and animals, composition of humic material strongly depends on its origin, extraction procedure and purification treatment. [8]

They constitute a substantial fraction of the organic matter in soils, sediments, water, and organic amendment materials such as composted urban solid waste or composted sewage sludge. HS are fractionated as Humin, Humic acids (HA) and Fulvic acids (FA). HA are defined as humic substances of high molecular weight and high chemical heterogeneity, the fraction that is soluble in alkaline solution but insoluble at pH <2, where as humin is the insoluble fraction and Fulvic acids (FA) is the fraction of humic substances that is soluble in water under all pH conditions. These molecules are known to be heterogeneous polyacids with polymeric structure constituted by different types of functional groups. These substances contain appreciable concentration of acidic functional groups, most of which are carboxylic and phenolic acids. [9]

Characterization of the HS molecular sizes, weights, structural arrangements and functional groups is essential for an adequate understanding of their varied role in the environment. Despite intense research on HS during the past decades, the molecular structure of humic and fulvic acids is not fully understood . Their study has generated lot of questions and to date there is still debate on HA structure and whether they are natural products. Indeed there is an argument that HA are man-made macromolecular species rather than natural product, that humic substances may be collections of diverse, relatively low molecular mass components forming dynamic associations stabilized by hydrophobic interactions and hydrogen bonds [9, 10].

In order to have a deeper understanding of these molecules there have been efforts to synthesize HA and FA. Various synthetic pathways such as abiotic oxidation, enzymatic, oxidative and radical polymerizations have been used [11]. Among the different starting materials that have been used include catechol (*o*-diphenol) and other types of phenols, glutamic acid, xylose, proteins or amino acids like glycine and triglycine. [11]

The aim of this study is to present a systematic study on the synthesis of humic and fulvic acids as a function of nature of the functional groups and thereafter characterize them by ATR-FTIR and UV-Visible spectroscopy. Synthesis at pH 5.5 is carried out using catechol, C_6H_5OH and acetic acid, CH_3COOH as starting materials. Catechol is an excellent starting material for oxidative polymerization since it is the simplest molecule containing the very reactive two hydroxyl groups in ortho-position, like other polyphenols in nature. Catechol has been found to polymerize in solution, both in ethanol and in water, leading to browning of the solution. Acetic acid is chosen as its one of the simplest carboxylic acid which will avail the carboxyl group. [11]

HA and FA were produced as evidenced by the spectroscopic (ATR-FTIR and UV-Visible) measurements,through polymerization reaction of catechol and acetic acid. The synthesis technique used is new andadvantageous as it's cheap and easy to undertake. Polymerization reaction is carried out at ambient conditions andduration of synthesis is relatively short. The reaction medium is not saturated with oxygen. The reactants areinexpensive and easily available. Following the spectroscopic data, it can be concluded that all fulvic acids <1,000 MWCO are more or less thesame in their chemical composition where as humic acid, fraction > 10,000 MWCO is probably characterized by aheterogenic chemical environment.[11]

Experimental

1. Materials

The starting chemicals were of analytical grade and used without further purification.

2. Physical and spectroscopic techniques

The characterization of the ligands and their corresponding metal complexes carried out using various spectroscopic techniques such as :-

i. Elemental analyses

Elemental analyses (C, H, N and Cl) were performed by analytical laboratory of Cairo University, Egypt.

ii. Molar conductivity

The molar conductivity of 10^{-3} M of metal complexes in dimethyl-sulfoxide (DMSO) was determined using Bibby conductimeter MCI at room temperature. The molar conductivities were calculated according to the following equation:

$\Lambda M = V*K*g/M_w*\Omega$

Where: Λ_M = molar conductivity ($ohm^{-1}\ cm^2\ mol^{-1}$)

V = volume of the solution (100 cm^3)

K = cell constant: 0.92 cm^{-1}

M_w = molecular weight of the complex

g = grams of complex dissolved in 100 cm^3 solution

Ω = resistance measured in ohms

iii. Mass spectra

The mass spectra of the ligand and their metal complexes were recorded on JEOL JMS-XA- 500 mass spectrometer.

iv. Thermal analyses

DTA and TGA were carried out on a Shimadzu DT-30 thermal analyzer in nitrogen atmosphere, from room temperature to 600 °C at a heating rate of 10 °C per minute.

v. ^{1}H- NMR spectra

The ^{1}H-NMR spectra were recorded on a JEOL EX -270 MHZ FT- NMR spectrometer in deuterated dimethylsulfoxide (DMSO- d6) as a solvent. The chemical shifts were measured relative to the solvent peaks.

Vi. IR spectra

The infrared spectra of solid ligands and their metal complexes were recorded on PerkinElmer's infrared spectrometer 681 using KBr or CsBr discs.

vii. Electronic absoption spectra

The electronic absorption spectra of the ligands and their complexes were recorded on UNICO SQ-4802 UV/ Vis. double beam spectrophotometer (190- 1100 nm) using 1 cm quartz cell using DMSO as a solvent.

viii. Magnetic susceptibility

The magnetic susceptibilities of the solid complexes in the solid state were measured in a borosilicate tube with a Johnson Matthey [12]. Magnetic susceptibility Balance at room temperature using the following equations:

$X_a = [2.086\ L\ (R- R^o) / (10^9 W)]$

$X_m = X_a * Mw$

$X_n = X_m - D$

$\mu_{eff} = 2.828\ (X_n \times T)^{1/2}$

Where:-

X_a = mass susceptibility

L = sample length in cm

R = tube + sample reading

R^o = empty the reading

W = mass of the sample

X_m = molar susceptibility

Mw = molecular weight

X_n = corrected molar susceptibility

D = diamagnetic corrections

μ_{eff} = effective magnetic moment

T = room temperature in Kelvin

The theoretical effective magnetic moment value calculated using the equation:

$\mu eff = [n(n+2)]^{1/2}$

Where:

μ_{eff} = theoretical effective magnetic moment

n = the number of the unpaired electrons diamagnetic corrections were made- by interpretation of Pascal's constant.

ix. Determination of metal content

Metal content was determined using colorimetric method on HACH DR 5000 spectrophotometer.

iix. ESR spectra

The solid ESR spectra of the complexes were recorded with ELEXSYS E500 Bruker spectrometer in 3 nm Pyrex Tubes at 25 °C. Diphenylpicr-hydrazide (DPPH) free radical was used as a g- marker for the calibration of the spectra. The equation used to determine g- values was

$g = (g_{DPPH})\ (H_{DPPH}) / H$

Where: $g_{DPPH} = 2.0036$

H_{DPPH} = magnetic field of DPPH in gauss

H = magnetic field of the sample in gauss

EXPERIMENTAL

3.1 FULVIC ACID EXTRACTION

Extracted fulvic acid was prepared from the raw material leonardite. The process was carried out as follow: hydrochloric acid (0.1M) was added to leonardite with stirring the suspension at 60 °C for one hour, then filtered off. The solid residue has been washed with H_2O several times. The obtained filtrate was distilled under vacuum to get fulvic acid as a light brown precipitate,

Ligand **(1)**

3.2 PREPARATION OF METAL COMPLEXES OF FULVIC ACID

Complex (2): nickel(II) sulfate hexahydrate (7.89g, 3 mol) dissolved in distilled water warmed at 60 °C was added to fulvic acid (6.38g, 1 mol) in the same solvent. The mixture was warmed at 60 °C with stirring for 30 min, then the solution was filtered off and yellowish green precipitate was obtained by evaporated the solution.

Complex (3): Copper(II) acetate monohydrate (5.98g, 3 mol) was added to fulvic acid (6.38g, 1 mol) using the above procedure.

Complex (4): Cobalt(II) acetate tetrahydrate (7.47g, 3 mol) was added to fulvic acid (6.38g, 1 mol) using the above procedure.

Complex (5): Copper(II) sulfate pentahydrate (7.47g, 3 mol) was added to fulvic acid (6.38g, 1 mol) using the above procedure.

Complex (6): cadmium(II) sulfate hydrate (23.1g, 3 mol) was added to fulvic acid (6.38g, 1 mol) using the above procedure.

Complex (7): manganese(II) acetate tetrahydrate (7.35g, 3 mol) was added to fulvic acid (6.38g, 1 mol) using the above procedure.

4. PREPARATION OF FULVIC ACID DERIVATIVES AND THEIR METAL COMPLEXES

4.1. PREPARATION OF FULVIC HYDRAZIDE LIGAND 2 (8)

fulvic hydrazide was prepared by adding 3drops of H_2SO_4 to one mole of fulvic acid(6.38g, 1.0 mol) in 50 cm^3 of methanol. The mixture was refluxed on water bath for 1 hour and then left to cool at room temperature, filtered off, then added (6.0 mols) hydrazine hydrate to the filtrate , the light brown precipitate was obtained, filtered off ,washed with methanol and dried.

4.2. PREPARATION OF METAL COMPLEXES OF FULVIC HYDRA-ZIDE

Complex (9): Copper(II) acetate monohydrate (3.0 mol) dissolved in distilled water warmed at 60 ^oC was added to fulvic hydrazide (1.0 mol) in the same solvent. The mixture was warmed at 60 ^oC with stirring for 30 min, then the solution was filtered off and the obtained deep olive precipitate was obtained by evaporated solution.

Complex (10):ferrous(II) sulphate heptahydrate (3.0 mol) was added to fulvic hydrazide (1.0 mol) using the above procedure

Complex (11):calcium(II) acetate (3.0 mol) was added to fulvic hydrazide (1.0 mol) using the above procedure

Complex (12):magnesium(II) acetate tetrahydrate (3.0 mol) was added to fulvic hydrazide (1.0 mol) using the above procedure

Complex (13): manganese(II) acetate tetrahydrate (3.0 mol) was added to fulvic hydrazide (1.0 mol) using the above procedure

4.3. PREPARATION OF THE LIGAND 3 (14)

The ligand [HL], fulvic hydrazide was prepared by adding equimolar amount of fulvic hydrazide (1.0 mol) to salicyaldehyde (1.0 mol) in 50 cm^3 of absolute ethanol. The mixture was stirred for 30 minutes. After cooling, the solvent was removed under reduced pressure to give crude product which was crystallized in ethanol to yield pure ligand **(3).**

Complex (15): Copper(II) acetate monohydrate (3.0 mol) dissolved in distilled water warmed at 60 ^oC was added to ligand **(3)** (1.0 mol) in the same solvent. The mixture was warmed at 60 ^oC with stirring for 30 min, then the solution was filtered off and the obtained deep olive precipitate by evaporated solution.

5-ANTIMICROBIAL ACTIVITY

Antimicrobial activity of the tested metal complexes was assessed against gram positive bacteria (*Streptococcus pneumonia* and *Bacillis subtilis*), gram negative bacteria (*Pseudomonas aeruginosa* and *Escherichia coli*) and fungi (*Aspergillus fumigates* and *Candida albicans*) by disc diffusion method **[13,14]**. Tetracycline was used as a positive control and solvent control (12mm) was also used to know the activity of the solvent. The test compounds were dissolved in DMSO to concentrations of 250, 200, 175, 150 and 125 ppm and a DMSO poured disc was used as negative control. The bacteria were sub cultured in nutrient agar medium, which was prepared using peptone, beef extract, NaCl, agar and distilled water. The Petri dishes were incubated for 48hrs at 37°C. The standard antibacterial drug tetracycline was also screened under similar conditions for comparison. The zone of inhibition was measured in millimeters carefully. All determination was made in duplicate for each of the compounds. An average of the two independent readings for each compound was recorded.

RESULTS AND DISCUSSION

I. PREPARATION AND INVESTIGATION OF FULVIC ACID AND ITS DERIVATIVE COMPLEXES:

The elemental analyses, spectral data (Tables 1-5) and thermal analyses (Table 6) reveal that, the complexes are formed in (1:3) (L:M) stoichiometric ratios. The complexes are colored, stable in air; soluble in polar solvents such as DMF and DMSO and ethanol, $CHCl_3$ and benzene. All the complexes are non-electrolytes. Many attempts were made to grow diffract able crystal, but unfortunately no crystal has been obtained until now. The preparation of ligands (2) and (3) are shown in *scheme 1.* The reaction of ligand (1) with metal ions in water led to the formation of complexes (2)-(7).The reaction of ligand (2) with metal ions in water led to the formation of complexes (9)-(13). The reaction of ligand (3) with metal ions in ethanol led to the formation of complexes (15).

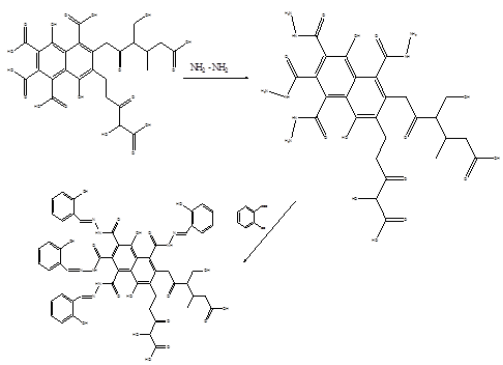

Scheme (1). Preparation of Ligands 2 and 3

No.	v(H2O/OH)	v(NH)	V(C-OH)	V(NH2)	v(C=O)	v(C=N)	v(Ar) / **(C=C)al	v(H-bond.)	v(OAc)/SO4	u(M-O)	u(M-N)	-
(1)	3465-3446 3385	-	1325	-	1665,1635	-	1433,872	3600-3310 3300-2650	-	-	-	-
(2)	3465-3440 3365-3315-3310-3030	-	1318	-	1650,1630	-	1440, 830	3610-3320 3310-3000	1140,1094 850,650	620	-	-
(3)	3470-3400 3365-3220 3210-3010	-	1280	-	1660,1628	-	1443,850	3585-3350 3340-2985	1570,1400	625 550	-	-
(4)	3468-3410 3370-3217-3200-2980	-	1285	-	1658,1620	-	1425,855	3620-3330 3320-2870	1572,1346	614 585	-	-
(5)	3463-3440 3200-3000	-	1315	-	1652,1632	-	1434,860	3585-3310 3300-2820	1138,1105 880,670	623	-	-
(6)	3465-3438 3170-3000	-	1315	-	1653,1630	-	1432,880	3570-3300 3290-2920	1138,1107 850,650	595	-	-
(7)	3465-3415 3180-2970	-	1182	-	1650,1630	-	1424,870	3590-3315 3300-2980	1568,1350	615 590	-	-
(8)	3400-3380	3260	1319	3313,3290	1655,1638	-	1503,790	3550-3320 3310-2650	-	-	-	-
(9)	3400-3378 3170-3000	3255	1316	3300,3280	1657,1630	-	1439,875	3535-3310 3300-2880	1425,1320	615 575	560	-

No.	v(H2O/OH)	v(NH)	V(C-OH)	V(N-N)	v(C=O)	v(C=N)	v(Ar) / **(C=C)al	v(H-bond.)	v(OAc)/SO4	u(M-O)	u(M-N)	-
(10)	3395-3380 3200-3000	3255	1317	3300,3275	1655,1631	-	1525,853	33520-3300 3290-2450	1167,1077 877,670	610	555	-
(11)	3400-3390 3360-3210 3200-3000	3250	1316	3285,3270	1558,1630	-	1500,878	3520-3310 3300-2760	1416,1310	605	561	
(12)	3395-3390 3180-2985	3250	1312	3300,3280	1650,1630	-	1581,850	3580-3310 3300-2720	1425,1310	617	563	-
(13)	3400-3388 3270-3020	3252	1311	3305,3290	1652,1629	-	1573,876	3560-3285 3280-2690	1420,1310	610	558	-
(14)	3450-3400	3250	1320	-	1660,1635	1610	1482-878 1428-748	3520-3220 3210-2750	-	-	-	-
(15)	3448-3395 3180-3000	3250	1318	-	1650,1630	1585	1480-828 1435-780	3535-3315 3310-2700	1510,1375	619	590	

A. MASS SPECTRA:

The mass spectrum of the free ligand (1), Table (3,a) revealed a molecular ion peak (m/z) at 638 a.m.u which is coincident with the formula weight of the ligand and supports the identity of the Structure. Furthermore, the fragments observed at m/z = 64, 80, 149, 195, 272, 381, 406, 461, 500, 544 and 638 corresponding to C_5H_4, C_5H_4O, $C_8H_5O_3$, $C_9H_7O_5$, $C_{10}H_8O_9$, $C_{15}H_9O_{12}$, $C_{17}H_{10}O_{12}$, $C_{20}H_{13}O_{13}$, $C_{23}H_{16}O_{13}$, $C_{25}H_{20}O_{14}$ and $C_{27}H_{26}O_{18}$ moieties respectively. The Co(II) complex (4),Table (3,b) spectrum show a peak (m/z) at 1058 a.m.u corresponding to the formula weight of the complex. Additionally, the peaks observed at 64, 77, 93, 109, 168, 204, 262, 366, 464, 547, 597, 655, 790, 906, 992, 1022 and 1058 are due to C_5H_4, C_6H_5, C_7H_9, C_8H_{13}, $C_{10}H_{16}O_2$, $C_{10}H_{20}O_4$, $C_{12}H_{22}O_6$, $C_{15}H_{26}O_{10}$, $C_{19}H_{28}O_{13}$, $C_{23}H_{31}O_{15}$, $C_{24}H_{37}O_{17}$, $C_{26}H_{39}O_{19}$, $C_{26}H_{40}Co_2O_{20}$, $C_{29}H_{40}Co_2O_{25}$, $C_{32}H_{42}Co_2O_{28}$, $C_{33}H_{44}Co_2O_{29}$ and $C_{33}H_{48}Co_2O_{31}$ moieties respectively.

Table (3,a):-Mass spectrum of the ligand (1), [H_2L].

m/z	Rel. Int.	Assignments
64	43	(C_5H_4)
80	96	(C_5H_4O)
149	6	($C_8H_5O_3$)
195	4	($C_9H_7O_5$)
272	3	($C_{10}H_8O_9$)
381	5	($C_{15}H_9O_{12}$)
406	5	($C_{17}H_{10}O_{12}$)
461	7	($C_{20}H_{13}O_{13}$)
500	7	($C_{23}H_{16}O_{13}$)
544	6	($C_{25}H_{20}O_{14}$)
638	32	($C_{27}H_{26}O_{18}$)

Table (3,b):- Mass spectrum of Co(II) complex (3).

m/z	Rel. Int.	Fragment
64	58	(C_5H_4)
77	73	(C_6H_5)
93	56	(C_7H_9)
109	57	(C_8H_{13})
168	82	($C_{10}H_{16}O_2$)
204	92	($C_{10}H_{20}O_4$)
262	92	($C_{12}H_{22}O_6$)
366	86	($C_{15}H_{26}O_{10}$)
464	81	($C_{19}H_{28}O_{13}$)
547	83	($C_{23}H_{31}O_{15}$)
597	89	($C_{24}H_{37}O_{17}$)
655	84	($C_{26}H_{39}O_{19}$)
790	87	($C_{26}H_{40}Co_2O_{20}$)
906	84	($C_{29}H_{40}Co_2O_{25}$)
992	82	($C_{32}H_{42}Co_2O_{28}$)
1022	82	($C_{33}H_{44}Co_2O_{29}$)
1058	87	($C_{33}H_{48}Co_2O_{31}$)

B. CONDUCTIVITY

The molar conductivity of 1×10^{-3} M solution of the metal complexes (1-15) in DMSO at room temperature are given in experimental section. The value of molar conductance of all complexes are in the 5.9-8.1 $\Omega^{-1}cm^2mol^{-1}$ range (Table 1), indicating a non-electrolytic nature of these complexes, confirming the involvement of the acetate, sulfate, nitrate and chloride anions in the coordination sphere.

C. INFRARED SPECTRA

Important spectral bands of the ligand and its complexes are presented in Table (2). The IR spectrum of the ligand showed broad medium intensity bands in the 3600–3310 and 3300-2650 cm^{-1} ranges, which are attributed to intra- and intermolecular hydrogen bondings [15-17]. The broad medium bands at 3465 and 3446cm^{-1} are assigned to the OH groups, whereas the relatively strong bands located at 1325 cm^{-1}, is assigned to the □(COH) [18,19]. In order to study the binding mode of the fulvic acid and its derivative to the metal ion in the complexes, the IR spectrum of the free fulvic acid was compared with the spectra of the metal complexes. The spectral data together with the elemental analyses indicated that, the ligand can behave as:

Neutral tetradentate ligand: coordinating through the one OHand the three C=O groups as in complexes (2),(5) and (6) . This mode of coordination is supported by the evidences: (i) the appearance of the band for the hydroxyl OH, Table (2) indicating at low value the coordination to the metal ion [20]. (ii) The strong bands observed around 1650 and 1630 cm^1, characteristic to the carbonyl (C=O) stretching vibrations were shifted to lower wave numbers, suggesting coordination of the carbonyl oxygen atoms to the metal ion [21-24]. (iii) The appearance of new bands in the 623-595 cm^{-1} regions which are assigned to υ(M-O) vibrations respectively [25]

Monobasic tetradentate ligand: As in complexes each of the two moieties of the ligand participating in the metal complexes coordinating through one O^- and three C=O groups as in complexes (3),(4) and (7), this mode of coordination was supported by the evidences: (i) the appearance of the band for the (C-O), Table (2) indicating at low value the coordination to the metal ion [20]. (ii) The strong bands observed around 1658 and 1620 cm^1, characteristic to the carbonyl (C=O) stretching vibrations were shifted to lower wave numbers, suggesting coordination of the carbonyl oxygen atoms to the metal ion [21-24]. (iii) The appearance of new two bands in the 625-550 , 614-585 and 615-590 cm^{-1} regions which are assigned to υ(M-O) vibrations respectively [25,26]. Neutral octadentate ligand: coordinating through tetra C=O and tetra NH_2group as in complexes (9),(10),(11),(12) and (13).This mode of coordination is supported by the following evidences:(i) the amine groups (NH_2) stretching vibrations were shifted to lower wave numbers, suggesting coordination of the amine nitrogen atoms to the metal ion [20]. (ii) The appearance of new bands in the 563-555cm^{-1} regions are corresponding to the υ(M-N) vibrations respectively [25].

Tetrabasic multidentate ligand: coordinating through tetra O^- , tetra amine and tetra C=O groups as in complex (15). This mode of coordination is supported by (i) vibration band of the C=N was shifted to lower wave number with a decreasing its intensity while the other one band appeared in its original place. [23,24]. (ii) The appearance of new bands in the 590 and 619 cm^{-1} regions are due to the υ(M-N) and υ(M-O) vibrations respectively [25]. (iii) The strong bands observed around 1650 and 1630 cm^1, characteristic to the carbonyl (C=O) stretching vibrations were shifted to lower wave numbers, suggesting coordination of the carbonyl oxygen atoms to the metal ion.

The presence of water molecules within the coordination sphere in all complexes were supported by the presence of weak bands around 3310-2980 cm^{-1} due to OH stretching, H_2O deformation, H_2O rocking and H_2O wagging, respectively [27, 28]. The appearance of two characteristic bands in the 1572-1346 , 1425-1310 and 1510-1375 cm^{-1} ranges in the spectra of complexes (3), (4), (7), (9), (11), (12), (13) and (15) were attributed to $\upsilon_{asym.}(COO^-)$ and $\upsilon_{sym.}(COO^-)$ respectively, indicating the participation of the acetate oxygen in the complex formation [29].

The coordination modes of the acetate group in the complexes were determined by IR spectra, by comparing the separations between the $\upsilon_{asym.}(COO^-)$ and $\upsilon_{sym.}(COO^-)$.The separation value□() between $\upsilon_{asym}(COO^-)$ and $\upsilon_{sym.}(COO^-)$ for these complexes (3), (4) and (7) , suggesting a tridentate coordination fashion of the acetate groups. Complexes (9), (11), (12) and (13), suggesting a octadentate coordination fashion of the acetate groups. Complex (15) suggesting a tetradentate coordination fashion of the acetate groups [30,31].

Complexesspectra demonstrated strong to medium bands at 1167-1077 and 877- 650 cm^{-1} belonging to the antisymmetric and symmetric stretching modes of the sulfate group. These values are consistent with that reported for the sulfate species coordinating to the M(II) in an bidentate fashion for complexes (2), (5) and (6) [14,32].

A. ELECTRONIC SPECTRA AND MAGNETIC MOMENT

DMF electronic absorption spectral bands as well as room temperature effective magnetic moment values of the ligand and its metal complexes are reported in (Table 4).The ligand showed three transition bands in the high energy region. The first band appeared at 290 nm which is assigned to $\pi\rightarrow\pi^*$ transition within

the aromatic rings and this band is nearly unchanged upon complexation. The second and third bands appearing at 315 and 350 nm may be assigned to $n\rightarrow\pi^*$ of the azomethine group and CT transitions [33,34].

The bands were found to be shifted upon complexation indicating involvement of these bands in coordination with the metal ions. The electronic spectra of the Co(II) complex (4) exhibit three transition bands at 445,580 and 625 nm. These bands are assigned to $^4T_{1g}(F)\rightarrow{}^4T_{2g}(F)(\nu_1)$, transitions respectively, corresponding to high spin cobalt(II) octahedral complexes [34,35]. The magnetic moments of complexes (4) is 5.23, which are well within the reported range of high spin octahedral Co(II) complexes. The electronic absorption spectra of Ni(II) complexe (1) displayed three bands at ranges, these bands are corresponding to $^3A_{2g}(F)\rightarrow{}^3T_{2g}(F)(\upsilon_1)$ transitions respectively, indicating octahedral nickel(II) complexes[36,37].

The magnetic moment values of nickel(II) complex (1) 3.13BM, which are consistent with two unpaired electrons state and confirming octahedral geometry around nickel(II) ions[36]. The electronic spectra of copper(II) complexes (3), (9) and (15) exhibited bands in the 605-620 and 575-590 nm ranges which are assigned to $^2B_{1g}\rightarrow{}^2A_{1g}$ $(d_{x^2-y^2}\rightarrow d_{z^2})$, and $^2B_{1g}\rightarrow{}^2E_g(d_{x^2-y^2}\rightarrow d_{xy},\ d_{yz})$ transitions respectively. These transitions indicate that, the copper(II) ion has a tetragonally distorted octahedral geometry. This could be due to the Jahn-Teller effect that operates on the d^9 electronic ground state of six coordinate system, elongating one trans pair of coordinate bonds and shortening the remaining four ones [17]. The electronic spectrum of complex (7) showed peaks at 525 and 575 nm. These bands are assigned to $^2B_1g\rightarrow{}^2B_2g$ and $^2B_1g\rightarrow{}^2A_1g$ transitions, indicating a square planar copper(II) complexes [24, 38].

The magnetic moments for all copper(II) complexes at room temperature are in the 1.29-2.6 B.M. range, indicating that, the complexes have octahedral or square planar geometry [39]. The apparent lower values of complexe (7) may be assigned to spin-spin interactions take place between copper (II) ions through molecular interactions [39]. The absorption spectra of manganese (II) complex (6) showed bands at 565, 620 nm. These two bands can be assigned to $^5B_{1g}\rightarrow{}^5E_g$ and $^6B_{1g}\rightarrow{}^6A_{2g}$ transitions respectively, suggesting an distorted octahedral arrangement around the manganese(II) ion [40,41].

Iron(II) complex (8) shows bands (Table 4) indicating octahedral structure [40]. The magnetic moment values for the complexes (6) are 4.25 B.M., which is consistent with a high spin octahedral geometry around the manganese(II) ion [40,42]. Iron(II) complexe (8) gave value 4.34 B.M., indicating octahedral structure [40]. Diamagnetic calcium(II) complex (9) showed only intraligand transitions and (LMCT).

Table (4):- Electronic Spectra (nm) and Magnetic Moments (B.M) for the

Ligands and their metal Complexes.

Comp. No.	λ_{max} (nm)	μ_{eff} (BM)	ν_2/ν_1
(2)	275,298,380,435,495,570, 615,720	3.13	
(3)	275,305,375,445,510,570, 618	2.6	-
(4)	280,298,310,370,445,580, 625	5.33	-
(7)	275,298,306,380,460,565, 620	4.25	-
(9)	280,310,395,465,525,575, 620	1.29	-
(10)	273,298,305,370,420,480, 575,630	4.34	-
(11)	265,280,305	Diama gnetic	-
(12)	275,298,305	2.1	-
(15)	280,298,305,385,465,580, 622	1.1	-

A. ELECTRON SPIN RESONANCE (ESR)

The ESR spectral data for metal complexes (3), (9) and (15) are presented in Table (5). The spectra of copper(II) metal complexes (9) and (15) are characteristic of species, d^9,configuration and having axial type of a $d(x^2-y^2)$ ground state which is the most common for copper(II) complexes [43,44]. The metal complexes showed $g_{||}>g_{\perp}> 2.03$, indicating octahedral geometry around the copper(II) ion [45]. The expression G is related to g-values, $G = (g_{||}-2)/ (g_{\perp}-2)$. If $G > 4.0$, then local tetragonal axes are misaligned parallel or only slightly misaligned and if $G < 4.0$, significant exchange coupling is present [46].

Metal complexes showed values indicating spin–exchange interactions takeplace between the copper(II) ions, which is consistent with the magnetic moments values(Table 4). Also, the $g_{||}/A_{||}$ values are considered as a diagnostic of stereochemistry. The $g_{||}/A_{||}$ values lie just within the range expected for the octahedral metal complexes [47]. The orbital reduction factors ($K_{||}$, $K_{\perp}$, K), which are a measure of covalence were also calculated [48]. K values, for the copper(II) complexes (9) and (15), indicating covalent bond character [48]. Also, the g-values show considerable a covalent bond character.

The in-plane σ- covalency parameter, α^2 (Cu) suggests a covalent bonding. The complexes show □ values indicating a covalency character in the in-plane □- bonding. While □ ² for the complexes indicating a covalent bonding character in the out of-plane □ bonding except complexes (9) and (15) which indicate ionic bond character [46,49]. The calculated orbital populations (a^2_d) for the copper(II) complexes indicate a d(x^2-y^2) ground state. Complex (3), show isotropic spectra.

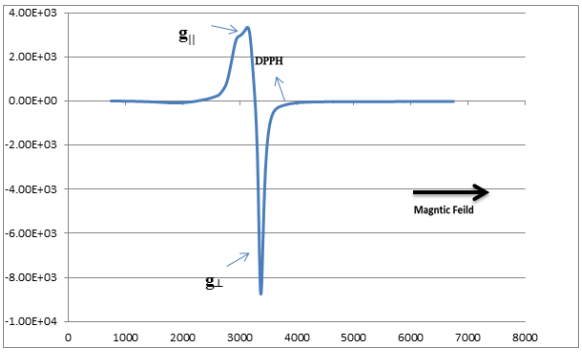

ESR spectrum of Cu(II) complex (15)

A. THERMALANALYSES(DTA AND TGA)

The thermal data of metal complexes (2), (3), (9) and (15) were presented in Table 6. The thermal curves in the 27-800°C temperature range indicated that, the metal complexes are thermally stable up to 40 °C. The weight losses recorded in the 70-90°C range is due to elimination of hydrated water molecules. Ni(II) complex (2) thermogram showed an endothermic peak at 45°C due to broken of the hydrogen bondings. An endothermic peak was observed at 80°C, with 3.14% weight loss (Calc. 3.29%) corresponding to loss of two hydrated water molecules. The endothermic peak observed at 155°C, with 5.24% weight loss (Calc. 5.38%) is due to loss of three coordinated water molecules. The endothermic peak observed at 230°C, with 9.79%weight loss (Calc. 10.12%) is due to loss of one terminal coordinated SO_4 group, whereas, the loss of the other terminal coordinated SO_4 group was accompanied by an endothermic peak at 250°C with 11.18% weight loss (Calc. 11.26 %). The endothermic peak observed at 310°C, is corresponding to melting point of the complex. Finally, the complex showed several exothermic peaks at 405, 420, 485, 510 and 530°C, with total 20.97% weight loss (Calc. 21.26%) corresponding to thermal decomposition with eventually formation of two NiO molecule. The thermogram of Cu(II) complex (3) showed an endothermic peak at 45°C is due to broken of hydrogen bondings. The endothermic peak observed at 75°C, with 3.49% weight loss (Calc. 3.49%) was assigned to loss of two hydrated water molecules. Whereas the endothermic peak observed at 145°C, with 8.4% weight loss (Calc. 8.7%) was ascribed to loss of a coordinated water molecule. Another endothermic peak was observed at 220°C, with 18.53%weight loss (Calc. 18.8%), which is assigned to loss of coordinated acetate group. The endothermic peak observed at 296°C, is corresponding to the melting point of the complex. The complex showed several exothermic peaks at 370, 410, 430 and 500°C, with total 20.27% weight loss (Calc. 20.7%) corresponding to thermal decomposition with the final formation of two CuO molecule. The thermogram of Cu(II) complex (9) showed an endothermic peak at 45°C due to broken of hydrogen bondings, whereas the loss of two hydrated water molecule was accompanied with endothermic peak at 80°C with 2.1% weight loss (Calc. 2.24%).The loss of coordinated water molecules was accompanied by two endothermic peaks at 140 and 150°C with weight losses 4.54% (Calc. 4.6%) and 4.89% (Calc. 4.82%) which were assigned to removal of four terminal and four terminal coordinated water molecules respectively. An endothermic peak was observed at 210,230°C with 32.86% weight loss (Calc. 33.2%) which could be assigned to loss of a coordinated acetate group. The endothermic peak observed at 304°C was assigned to the melting point of the complex. Thermal decomposition of the complex was accompanied by multiple exothermic peaks at 370, 410, 510, with total 33.42% weight loss (Calc. 33.48%) with final formation of four CuO molecules. The thermogram of Cu(II) complex (15) showed an endothermic peak at 45°C due to broken of hydrogen bondings, whereas the loss of two hydrated water molecule was accompanied with endothermic peak at 70°C with 1.73% weight loss (Calc. 2.02%).The loss of coordinated water molecules was accompanied by two endothermic peaks at 130 and 155°C with weight losses 4.16% (Calc. 4.13%) and 4.51% (Calc. 4.31%) which were assigned to removal of four terminal and four terminal coordinated water molecules respectively. An endothermic peak was observed at 225°C with 14.58% weight loss (Calc. 14.77%) which could be assigned to loss of a coordinated acetate group. The endothermic peak observed at 290°C was assigned to the melting point of the complex. Thermal decomposition of the complex was accompanied by multiple exothermic peaks at 370, 410, 470, with total 23.26% weight loss (Calc. 23.37%) with final formation of four CuO molecules.

Table (6):- Thermal analyses for metal (II) complexes.

Compound No. Molecular formula	Temp. (°C)	DTA (peak)		TGA (Wt.loss %)		Assignments
		Endo	Exo	Calc.	Found	
Complex (2) $C_{72}H_{80}N_{12}O_{25}S_2$	50	Endo	-	-	-	Broken of H-bondings
	80	Endo	-	3.29	3.14	Loss of ($2H_2O$) hydrated water molecules
	135	Endo	-	5.11	4.89	Loss of ($3H_2O$) coordinated water molecules
	155	Endo		5.38	5.24	Loss of ($3H_2O$) coordinated water molecules
	230	Endo		10.12	9.79	Loss of coordinated SO_4 group
	250	Endo		11.26	11.18	Loss of coordinated SO_4 group
	310	Endo	-	-	-	Melting point
	420	-	Exo	21.26	20.97	Decomposition process with the formation of2NiO

Complex (3) $C_{12}H_{44}Cu_2O_{28}$	45	Endo	-	-	-	Broken of H-bondings
	75	Endo	-	3.49	3.49	Loss of 2(H_2O) hydrated water molecules
	145	Endo	-	8.7	8.4	Loss of (5H_2O) coordinated water molecules
	220	Endo	-	18.8	18.53	Loss of coordinated 3(OAc) group
	295	Endo	-	-	-	Melting Point
	430	-	Exo	20.7	20.27	Decomposition process with the formation of 2CuO

Complex (9) $C_{81}H_{74}Cu_4N_8O_{38}$	45	Endo	-	-	-	Broken of H-bondings
	80	Endo	-	2.24	2.10	Loss of (2H_2O) hydrated water molecules
	140	Endo	-	4.6	4.54	Loss of coordinated(4H_2O) molecule
	155	Endo		4.82	4.80	Loss of coordinated(4H_2O) molecule
	210,230	Endo	-	33.2	32.86	Loss of coordinated 8(OAc) group
	304	Endo	-	-	-	Melting point
	370,410	-	Exo	33.48	33.42	Decomposition process with the formation of CuO

Complex (15) $C_{65}H_{74}Cu_4N_8O_{34}$	45	Endo	-	-	-	Broken of H-bondings
	70	Endo	-	2.02	1.73	Loss of (2H_2O) hydrated water molecules
	130	Endo	-	4.13	4.16	Loss of (4H_2O) coordinated water molecules
	155	Endo	-	4.31	4.51	Loss of (4H_2O) coordinated water molecules
	225	Endo	-	14.77	14.58	Loss of coordinated 4(OAc) group
	290	Endo	-	-	-	Melting point
	410	-	Exo	23.37	23.26	Decomposition process with the formation of 4CuO

II. APPLICATION OF FULVIC ACID METAL COMPLEX AND ITS DERIVATIVES

A. ANTIMICROBIAL ACTIVITY

In vitro biological screening tests of the ligand and its metal complexes (3), (9), (10),(11),(12) and (15) carried out as antibacterial and antifungal activity and presented in (Table 7) and chart (38). The antibacterial activity was tested against two bacterial strains; Gram-positive *Streptococcus pneumonia* (*S. pneumonia*) and *Bacillis subtilis* (*B. subtilis)* as well as Gram-negative *Escherichia coli (E.coli)* and *Pseudomonas aeruginosa (P. aeruginosa)* strains. The results compared with standard drug (Ampicllin (Gram positive) and Gentamicin (Gram negative). The data indicated that, complexes were active against bacteria. Cu(II) Complexes (3) , (9) and (15) and Fe(II) complex (10) and Ca(II) complex (11) and Mg(II) complex (12) with fulvic acid and its derivative show antibacterial activities against *S. pneumonia* , *B. subtilis, E.coli* and *P. aeruginosa* [50,51]. Also the results showed that, the order of cytotoxic effect against Gram positive and Gram negative strains for *S. pneumonia* is standard > (3)> (12) > (11) > (9) > (10) > (15) , for *B. subtilis* the order is as standard > (12) > (11) > (3) > (9) > (10) > (15). Also for *E.coli* the order is standard > (12) > (11) > (15) > (9),(10) > (3). Also for *P. aeruginosa* the order is standard > (12) > (11) > (15) > (3) > (9) > (10). The complexes were also subjected to antifungal activity against *Aspergillus* fumigatus *(A.* fumigatus*)* and *Candida albicans (C. albicans)*. The investigation shows that, all tested complexes in general have more activity than the parent ligand against *A.* fumigatus but inactive against *C. albicans*. Analysis of growth pattern of *A.* fumigatus in the presence of complexes reveals that, the complexes have potential to inhibit the growth of fungus tested. Further, the complexes are more active than the free ligand, which indicates that, metalation increases antimicrobial activity. Cu(II) complex (3) and Mg(II) complex (12) are more active against *C. albicans*. The complexes of hydrazide derivative are more active for microorganisms and this is also indicates that, nitrogen is a more effective antimicrobial agent. On comparing the results in general, it may be concluded that, the complexes have greater inhibiting power than the free ligand against all the microbes tested. The zone of inhibition was measured with respect to control.

Table(7):Biological activities of the ligand and its metal complexes(3),(9),(10),(11),(12)and (15) against bacteria and fungus

Compounds	Inhibation zone in mm					
	S. pneumoniae	*B. subtilis*	*P. aeruginosa*	*E. coli*	*A. fumigatus*	*C. albican*
Standard drug	23.8	32.4	17.3	19.9	23.7	19.7
DMSO	0	0	0	0	0	0
(3)	13.8	12.4	11.3	9.9	13.7	19.7
(9)	10.2	12.3	10.1	10.3	11.3	12.2
(10)	10.1	10.9	8.7	10.3	0	0
(11)	12.6	13.7	13.1	11.3	14.3	10.6
(12)	13.7	14.9	13.8	12.1	11.7	18.1
(15)	9.5	9.8	12.3	10.6	12.3	10.5

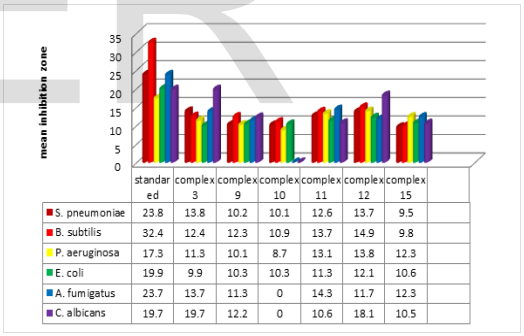

Mean inhibition zone of the ligand and metal complexes (3), (9), (10), (11), (12)and (15) against Aspergillus Funigatus, Streptococcs pneumoniae, Bacillis Subtilis, and Escherichia coli, pseudomonas aerginosa and candida Albicans

.

A. EVALUATION OF PLANT GROWTH PROMOTION OF FULVIC ACID AND DERIVATIVES CHLEATES

The fulvic acid chelates were evaluated for plant growth promoter on (pepper) plant. Results indicated that, the growth criteria like plant height, stem diameter, leaves area, number of flowers, number of branches, and total yield per plant were improved by increasing dose of the organically chelated fulvic acid to a concentration of 3% of mixture fulvic acid and its derivative metal chelates.

Height at this concentration the plants recorded the maximum height (58.7 cm), while plant recorded height (55.6 cm) when the fulvic acid chelates was foliarly applied to the plant at 2 % concentration. Treating plants with unchelated metal nutrient solution 3% produced plants with (50.56 cm). The least plant height (45.6 cm) was recorded upon treating the plant with the control.

Number of branches per plant was maximum (16.27) using 3% fulvic acid chelates chelate as a foliar spray. It was followed by 2% foliar spray of fulvic acid chelates with (13.58) branches per plant. Whereas foliar spray of unchelated metal nutrient solution at 3% produced (13.42) branches per plant and. The least number of branches per plant (11) was recorded using the control.

Growth characters like stem diameter of plants and leave area of plants were increased significantly with application of increased dose of fulvic acid chelated metal nutrients. Among the different treatments of chelated metal nutrients treatments; spraying plants with 3 % of the chelated metal by fulvic acid and derivative showed better results than the other treatments through improved characters of number of flowers per plant. The maximum number of flowers per plant 115.86 and 92.93flower/plant was recorded at 2% and 3 % treatment respectively while the control recorded 79.48 (flower/plant). The yield per plant was maximum (336.86 gm) with the spray of 3 % of potassium fulvate and fulvic acid micronutrient .

Table(8):Effect of foliar application of untreated control T_0, 3% micro-nutrient solution T_1, 2% fulvic acid micronutrient T_2, 3% potassium fulvate and fulvic acid micronutrient T_3.

Treatment	Average of Plant height (cm)	Second Leave area (mm)	Yield per plant (gm)	Branches Number	Number of flowers
T_0	45.6	176.93	231.5	11	79.48
T_1	50.5	211.97	309	13.42	91.13
T_2	55.6	214.03	322.6	13.58	92.93
T_3	58.7	231.50	336.86	16.27	115.86

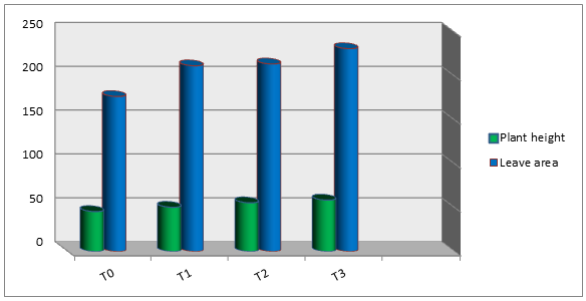

Chart (39):- Plant height and leave area of pepper plant using fulvic acidand its derivatives chelates

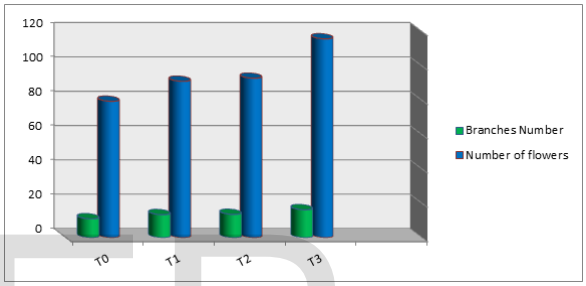

Chart (40)- Number of branches and number of flowers of pepper plant using fulvic acid and its derivatives chelates

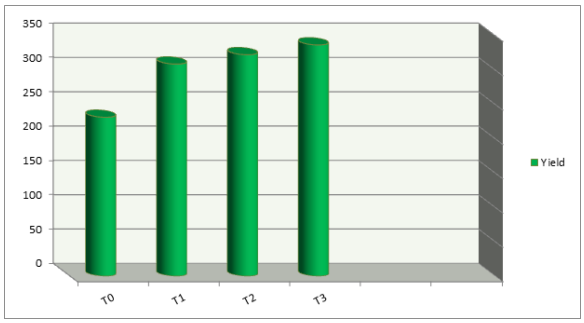

Chart (41):- Yield per plant of pepper plant using fulvic acid and its derivatives chelates

Figure(20):- foliar application untreated control T_0

Figure(21):- foliar application 2% fulvic acid micronutrient T_2

Figure(22):- foliar application 3% fulvic acid micronutrient T_3

Conclusion

Spectroscopic (IR , UV-VIS, Mass and ESR spectra) and elemental studies of the ligand (H_2L) and its metal complexes were reported. The magnetic properties and thermal analyses (DTA and TGA) were also carried out. The IR spectra of the prepared complexes suggested that, the ligand adopted either a bidentate or a tetradentate fashion, bonding to the metal ion through the azomethine nitrogens and the two phenolic oxygen atoms (ONNO). Electronic spectra and magnetic susceptibility measurements revealed an octahedral geometry for all complexes. The elemental analyses and mass spectral data have justified the ML, ML_2, $M_2L$and M_3L_2 composition of the complexes. The ESR spectra of Cu(II) complexes (2), (7) and (12), showed an axial type (dx^2-y^2) ground state with a covalent bond character and also support the suggested structures of complexes.

The antimicrobial activity revealed the compounds recorded an activity against *Candida albicans* fungi . In contrary, it was found that most compounds exhibit antibacterial activity against the other tested types of microbes. complex (2) and (10) represented the most sensitive complex against *Candida albicans* fungi, whereas complex (10) recorded moderate activity against *Escherichia coli* and *Streptococcs pneumonia*.

Chelates evaluated as mixture for growth promotion and productivity ability of the organically chelated metal nutrients on pepper plant. The growth Characters like plant height, leaves area, number of flowers, number of branches per plants and total yield per plant was determined after last harvest.

REFERENCE

1) M. Eladia, P. Méndez, J. Havel, J. Patočka, J. Appl. Biomed. (2005),3: 13.24 .
2) M. I. Dinu, *Water Resources, (2010), Vol. 37, No. 1, pp. 65–69.*
3) B. A. Borisov, N. F Ganzhara, *Pochvovedenie*, (2008), no. 9, pp. 1071–1078 [*Eur. Soil Sci.* (Engl. Transl.) pp. 946–952].
4) L.Z. Granina, E.Kallender, , *Geokhimiya*, (2007), no. 9, pp. 999–1007 [*Geochem. Int.* (Engl. Transl.), no. 9, pp. 918–925].
5) A. A. Fedorov, G. Z. Kaziev, G. D. Kazakova, , Moscow: KolosS,(2007).
6) I.Y. Koshcheeva, S. D. Khushvakhtova, V. V. Levinskii, *Geokhimiya*, (2007), no. 2, pp. 208–215 [*Geochem. Int.* (Engl. Transl.), no. 2, pp. 185–192].
7) T. I. Moiseenko, L. N. Kudryavtseva, N. A. Gashkina, Moscow: Nauka, (2006).
8) A.K. Kiprop, M. C. J. Coumon, E. Pourtier, S. Kimutai, S. Kirui, *International Journal of Applied Science and Technology. Vol. 3 No. 8; (2013)*
9) R. Sutton, G. Sposito, *Environ. Sci. Technol.* (2005), *39*, 9009-9015.
10) P. Zuman, E. Rupp, *Croatica Chemica Acta* CCACAA (2006), *79*,57 65.
11) A. Jung, C. Frochot, S. Parant, B. Lartiges, C. Selve, M. Viriot, J. Bersillon, *Organic Geochemistry* (2005), *36*,1252-1271.
12) J. Lewis and R. Wilkens, "Modern Coordination Chemistry, Interscience Pub," *Inc, New York,* (1960)p. 403.
13) A. Nicodemo, M. Araujo, A. Ruiz, and A. Gales, *Journal of Antimicrobial Chemotherapy*, vol. 53, (2004) pp. 604-608.
14) M. S. Yadawe and S. A. Patil, *Transition Metal Chemistry*, vol. 22, (1997) pp. 220-224.

15) A. S. El-Tabl, M. M. Shakdofa, A. M. El-Seidy, A. N. Al-Hakimi, Phosphorus, Sulfur, and Silicon and the Related Elements 187(2012) 1312-1323.
16) P. Deveci, B. Taner, Z. Kılıç, A. O. Solak, U. Arslan, E. Özcan, Polyhedron 30(2011) 1726-1731.
17) D. Pavia, G. Lampman, G. Kriz, J. Vyvyan, Belmont, CA, USA(2009).
18) S. Naskar, S. Naskar, S. Mondal, P. K. Majhi, M. G. Drew, S. K. Chattopadhyay, Inorganica chimica acta 371(2011) 100-106.
19) I. Gulaczyk, M. Kręglewski, Journal of Molecular Spectroscopy 249(2008) 73-77.
20) I. Gulaczyk, M. Kręglewski, A. Valentin, Journal of Molecular Spectroscopy 220(2003) 132-136.
21) Singh G, Singh P, Singh K, Singh D, Handa R, Dubey N, Proc. Natl. Acad. Sci. Ind 72A(2002) 87.
22) H. H. Monfared, Z. Kalantari, M. A. Kamyabi, C. Janiak, Zeitschrift für anorganische und allgemeine Chemie 633(2007) 1945-1948.
23) O. Pouralimardan, A.-C. Chamayou, C. Janiak, H. Hosseini-Monfared, Inorganica Chimica Acta 360(2007) 1599-1608.
24) S. Kannan, R. Ramesh, Polyhedron 25(2006) 3095-3103.
25) D. Lin-Vien, N. B. Colthup, W. G. Fateley, J. G. Grasselli, Elsevier, 1991.
26) A. S. El-Tabl, W. Plass, A. Buchholz, M. M. Shakdofa, Journal of Chemical Research 2009(2009) 582-587.
27) E. Keskioğlu, A. B. Gündüzalp, S. Cete, F. Hamurcu, B. Erk, Spectrochimica Acta Part A: Molecular and Biomolecular Spectroscopy 70(2008) 634-640.
28) M. Teotia, J. Gurtu, V. Rana, Journal of Inorganic and Nuclear Chemistry 42(1980) 821-831.
29) M. Fouda, M. Abd-Elzaher, M. Shakdofa, F. El Saied, M. Ayad, A. El Tabl, Transition Metal Chemistry 33(2008) 219-228.
30) K. Nakamoto, , Wiley Online Library, 1978.
31) B. Murukan, K. Mohanan, Transition Metal Chemistry 31(2006) 441-446.
32) A. S. El-Tabl, F. A. El-Saied, A. N. Al-Hakimi, Synthesis, Transition Metal Chemistry 32(2007) 689-701.
33) K. Nakamoto, Wiley Online Library, 1986.
34) M. F. Fouda, M. M. Abd-Elzaher, M. M. Shakdofa, F. A. El-Saied, M. I. Ayad, A. S. El Tabl, Journal of Coordination Chemistry 61(2008) 1983-1996.
35) A. Lever, Electronic spectra of some transition metal complexes: Derivation of Dq and B, Journal of Chemical Education 45(1968) 711.
36) H. G. Aslan, S. Özcan, N. Karacan, Inorganic Chemistry Commu-nications 14(2011) 1550-1553.
37) G. G. Mohamed, M. Omar, A. M. Hindy, Spectrochimica Acta Part A: Molecular and Biomolecular Spectroscopy 62(2005) 1140-1150.
38) W. J. Geary, Coordination Chemistry Reviews 7(1971) 81-122.
39) Z. H. Chohan, C. T. Supuran, Applied organometallic chemistry 19(2005) 1207-1214.
40) M. Akbar Ali, A. H. Mirza, C. Y. Yee, H. Rahgeni, P. V. Bernhardt, Polyhedron 30(2011) 542-548.
41) K. R. Surati, B. Thaker, , Spectrochimica Acta Part A: Molecular and Biomolecular Spectroscopy 75(2010) 235-242.
42) K. R. Surati, Synthesis,Spectrochimica Acta Part A: Molecular and Biomolecular Spectroscopy 79(2011) 272-277.
43) B. J. Kennedy, K. S. Murray, Inorganic Chemistry 24(1985) 1552-1557.
44) B. J. Hathaway, D. E. Billing, Coordination Chemistry Reviews 5(1970) 143-207.
45) J. C. Eisenstein, the Journal of Chemical Physics 28(1958) 323-329.
46) A. A. G. Tomlinson, B. J. Hathaway, Journal of the Chemical Society A: Inorganic, Physical, Theoretical(1968) 1685-1688.
47) A. S. El-Tabl, F. A. Aly, M. M. E. Shakdofa, A. M. E. Shakdofa, Journal of Coordination Chemistry 63(2010) 700-712.
48) A. N. Al-Hakimi, A. S. El-Tabl, M. M. Shakdofa, Journal of Chemical Research 2009(2009).
49) N. M. Shauib, A.-Z. A. Elassar, A. El-Dissouky, Spectrochimica Acta Part A: Molecular and Biomolecular Spectroscopy 63(2006) 714-722.
50) N. N. Greenwood, B. P. Straughan, A. E. Wilson, Journal of the Chemical Society A: Inorganic, Physical, Theoretical(1968) 2209-2212.
51) B. Tweedy, Phytopathology 54, AMER PHYTO-PATHOLOGICAL SOC 3340 PILOT KNOB ROAD, ST PAUL, MN 55121, 1964, pp. 910

Complexes structure :

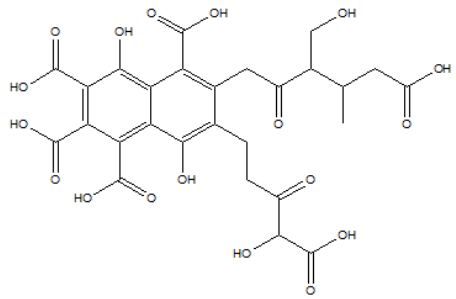

Ligand 1:Structure of Fulvic acid (1)

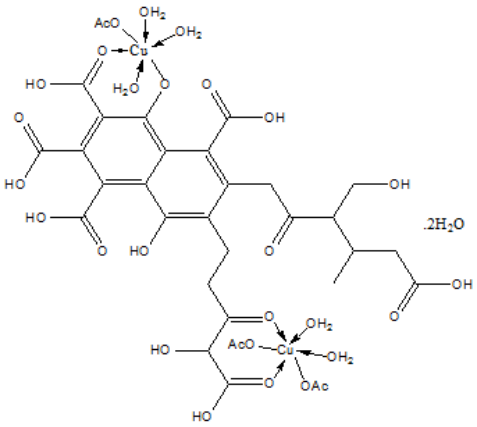

Structure of Cu(II) Complex (3)

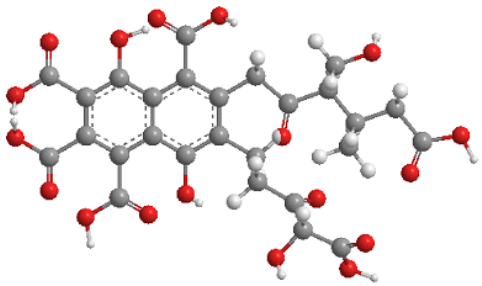

Structure of Fulvic acid (3D) (1)

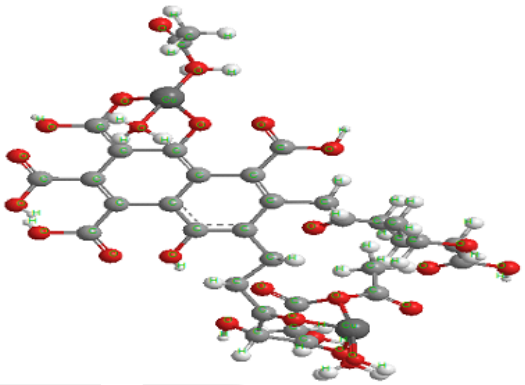

Structure of Cu(II) Complex (3) (3D)

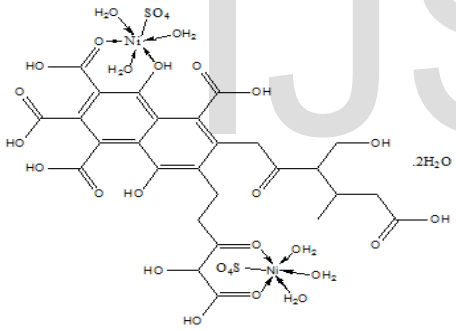

Structure of Ni(II) Complex (2)

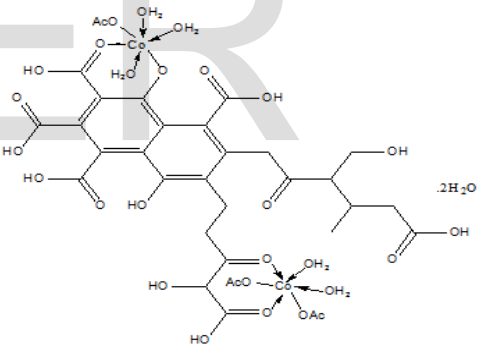

Structure of Co(II) Complex (4)

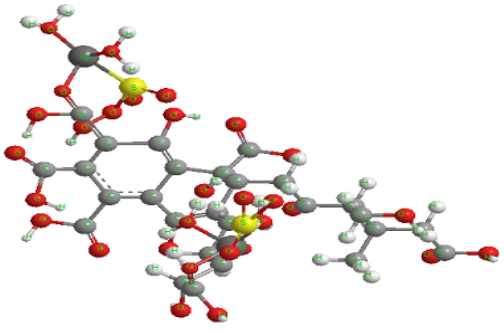

Structure of Ni(II) Complex (2) (3D)

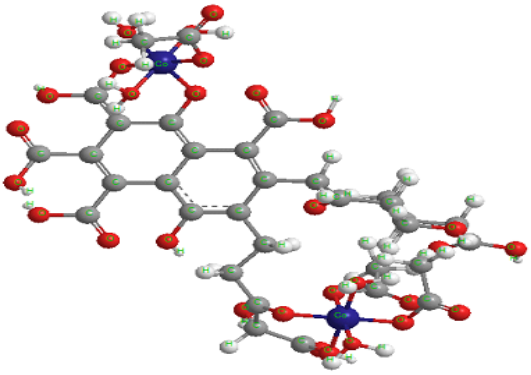

Structure of Co(II) Complex (4) (3D)

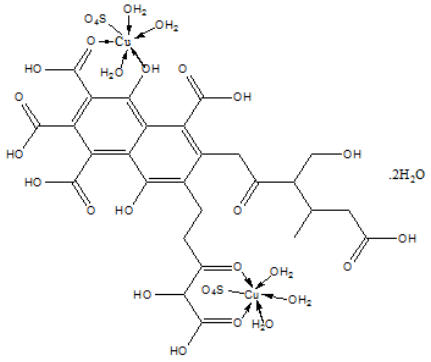

Structure of Cu(II) Complex (5)

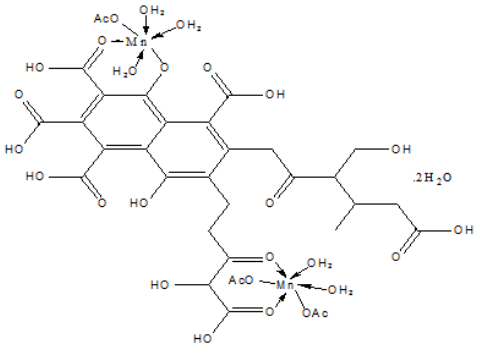

Structure of Mn(II) Complex (7)

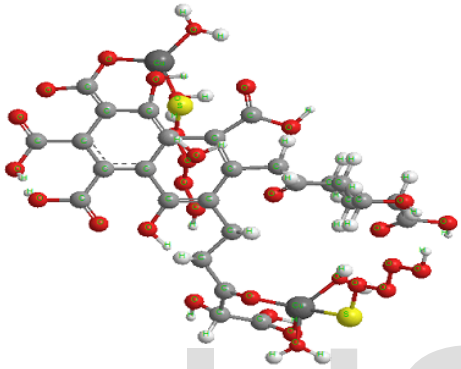

Structure of Cu(II) Complex (5) (3D)

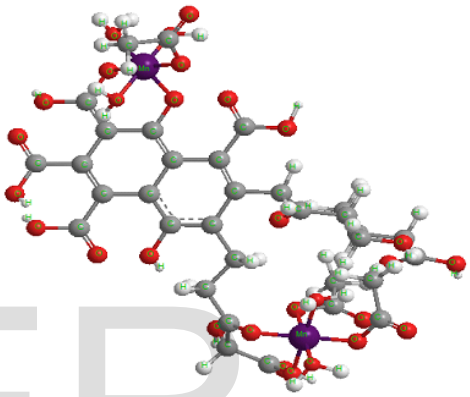

Structure of Mn(II) Complex (7) (3D)

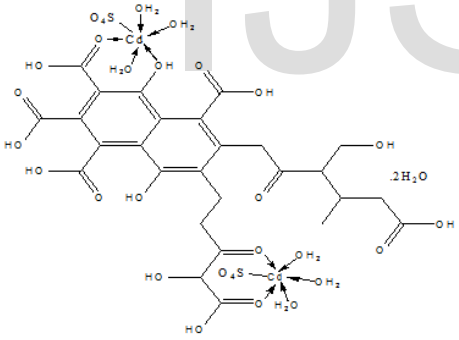

Structure of Cd(II) Complex (6)

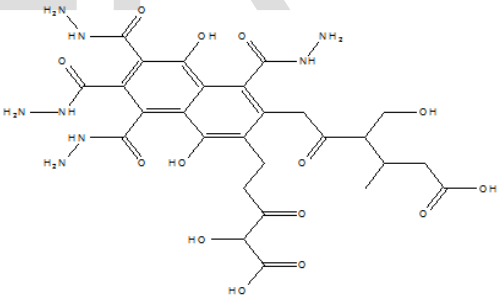

Structure of Ligand 2 (8)

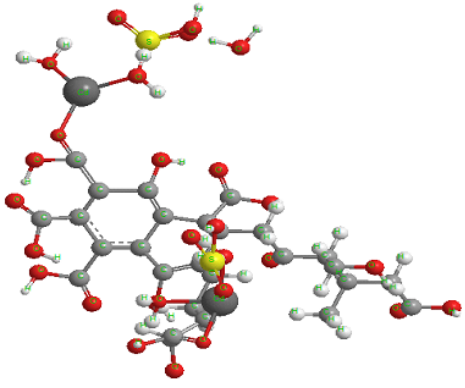

Structure of Cd(II) Complex (6) (3D)

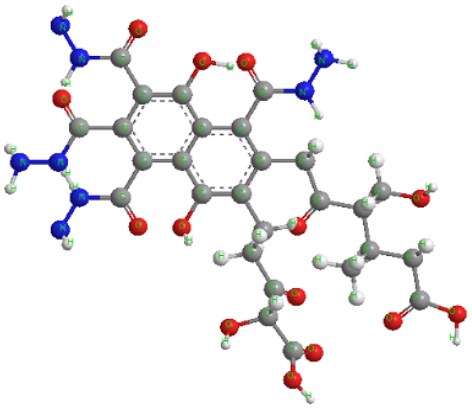

Structure of Ligand 2 (8) (3D)

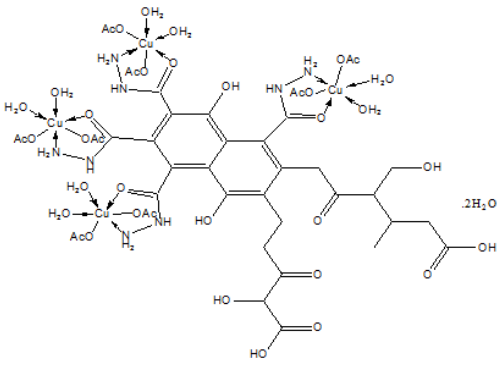

Structure of Cu(II) Complex (9)

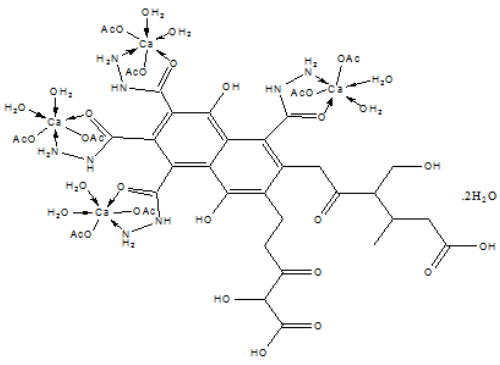

Structure of Ca(II) Complex (11)

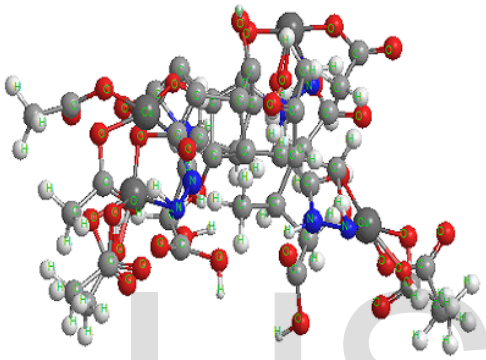

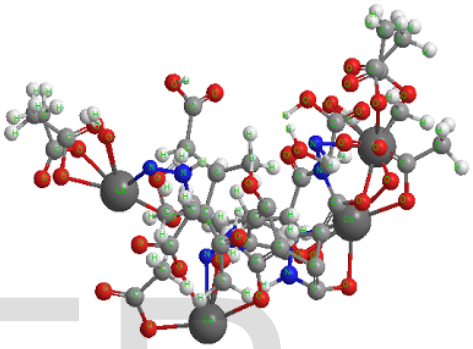

Structure of Ca(II) Complex (11) (3D)

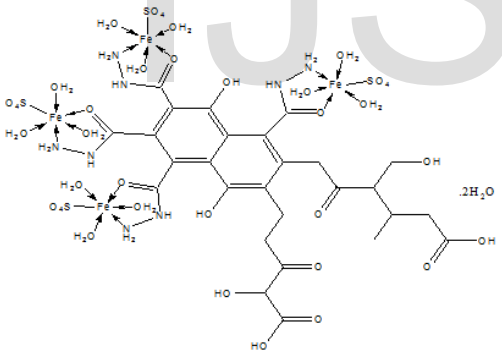

Structure of Fe(II) Complex (10)

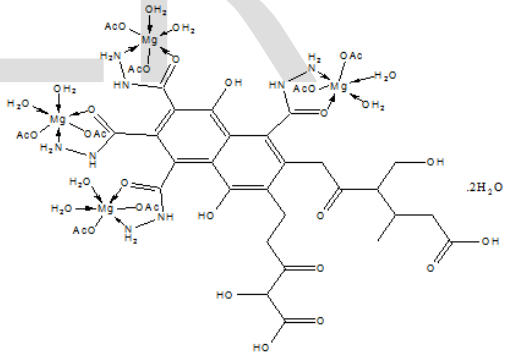

Structure of Mg(II) Complex (12)

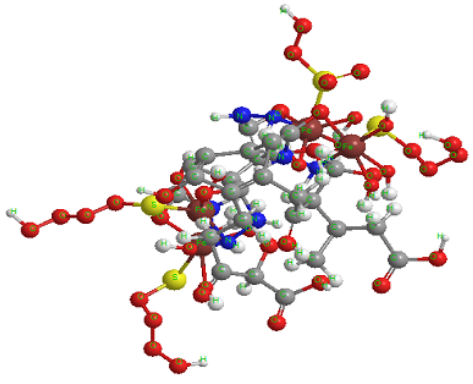

Structure of Fe(II) Complex (10) (3D)

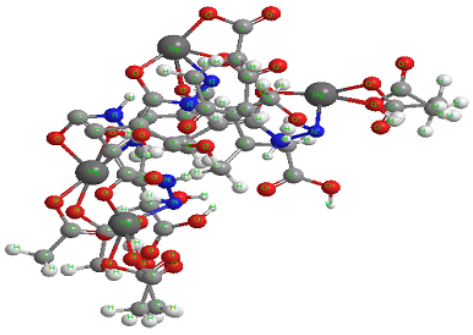

Structure of Mg(II) Complex (12) (3D)

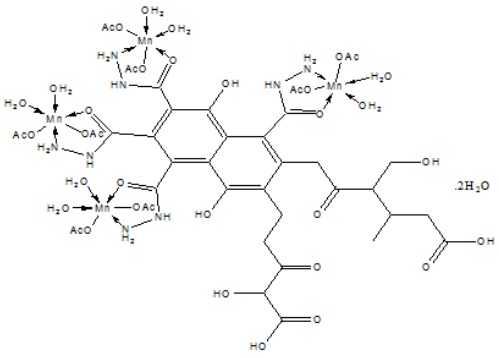

Structure of Mn(II) Complex (13)

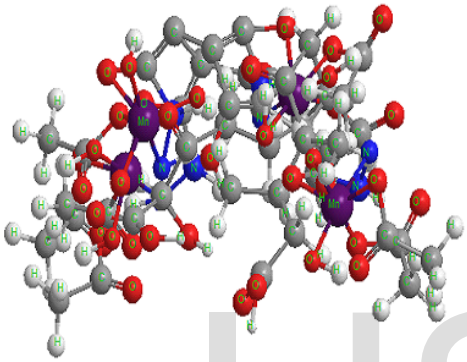

Structure of Mn(II) Complex (13) (3D)

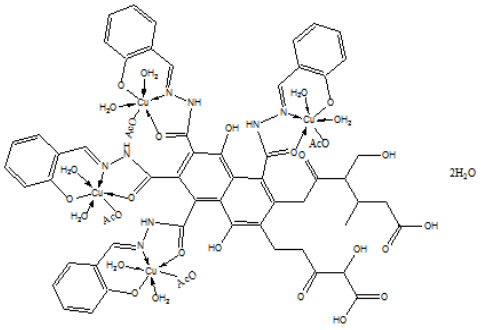

Structure of Cu(II) complex (15)

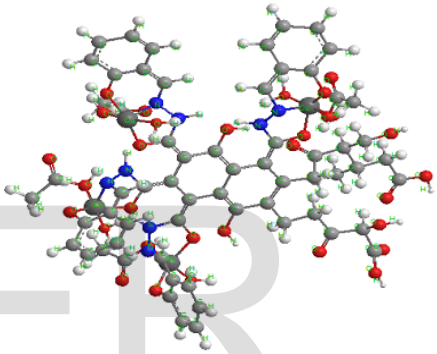

Structure of Cu(II) complex (15) (3D)

Suggested structure of the ligand and its metal complexes.

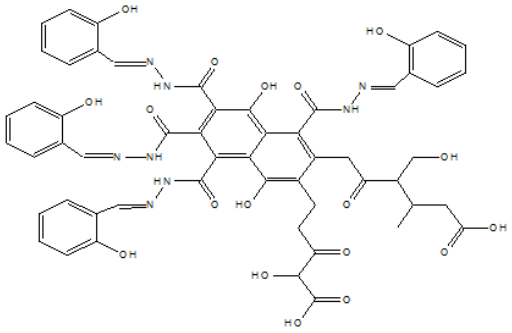

Structure of ligand 3 (14)